

A new analytical formula for calculating the energy gap value using the transmittance curve

H. Slimani^{1,2*}, N. Bessous²

¹University of El Oued, Faculty of Science, Department of Physics, El Oued, 39000, Algeria

²University of El Oued, Faculty of Technology, Department of Electrical Engineering, El Oued, 39000, Algeria

Received: March 02, 2020; Revised: September 24, 2021

This paper presents a new method to calculate the energy gap (E_g) value. The transmittance curve allows to define the E_g value. It is known that in a study, the calculation of the E_g may give a significant difference between two readings. These readings give a considerable overlap in the results to be analyzed, which is considered as a major drawback when different researchers' results are compared. The present paper proposes a new analytical model providing a unified formula to define the energy gap value. This new formula is based on logical analytical development and allows to guarantee the variation between the different energy gap values. As examples, thin films of zinc oxide (ZnO) and nickel oxide (NiO) on fluorine-doped tin oxides (FTO), used in photovoltaic system applications, are given.

Keywords: Ultraviolet-visible spectroscopy, energy gap, thin layer, analytical model, transmittance curve.

INTRODUCTION

A thin film is an entity with extremely small geometrical dimensions (thickness from a few tens of nm to a few μm). This explains why the physical features of these items are so important in surface interactions [1-7]. Moreover, this is the main reason why the physical properties of thin films significantly differ from those of other structures. In general, thin films are used in many applications such as photovoltaic systems, photocatalysis, optic systems, nano-electronics, etc. [8-14]. Microscopically, they consist of crystalline grains which are of the same order of magnitude as the thickness of the thin layer [15-17]. According to the literature, the thin layers have a microstructure in the form of columns with diameters ranging from 10 to 30 nm [18]. The orientation of the crystalline grains varies as a function of the angle between the plane of the substrate and the flow of molecules during the deposition [19-21].

The chemical and physical qualities of any material, as well as the physical conditions of deposition at each stage of the thin layer evolution have a huge impact on the microstructure of thin layers. In particular, the properties of a thin layer are very sensitive to the nature of the substrate on which it is located. This explains why layers of the same material and the same thickness may have substantially different physical properties on substrates of different types [22-24].

There are many techniques for deposition of thin layers on substrates [25-27]. The use of a technique depends on the properties of the deposited layers for a given application.

According to the theory of energy bands, there are three electrical states: metal, insulator and semiconductor. In the metal, the conduction band (CB) and the valence band (VB) are overlapping, which allows a free flow of the electrons. The semiconductor has a forbidden band that separates the VB and the CB, commonly called gap, and noted as E_g . The electrons cannot take the energies located in this band. They need to gain energy to get into the CB. For insulators the energy gap is larger than 4 eV, and at room temperature, the CB of an insulator is empty.

Glasses are common amorphous (not crystallized) materials, transparent in the visible range. They have a very high gap value and cannot conduct electric current (insulator).

However, semiconductors with a large gap (at least above 3.1 eV, corresponding to a wavelength of 400 nm) are theoretically transparent in the visible range. Thin layer deposition of this type of material ensures low absorption. The presence of admixtures, introduced by doping of the material, increases the number of free electrons.

Zinc oxide (ZnO) is a semiconductor of wide gap; it is transparent in the visible and in the near infrared range. It possesses a set of properties that allow its use in many applications [28-30]. It has very interesting electromechanical properties which allow its usage on a large scale as a transparent conductor in acoustic devices and in microwave delay lines, as piezoelectric materials, etc.

Different quantitative data are obtained by chemical analysis based on ultraviolet-visible (UV-Vis) spectroscopy. Transition metal ions, biological

* To whom all correspondence should be sent:
E-mail:slimani_hamza@yahoo.fr

macromolecules, highly conjugated organic compounds, etc., are used as dopants. UV-Vis spectroscopic measurements can also be performed in solids and in gases.

This technique is usually applied to molecules and/or inorganic complexes in solution. The perceived color of the chemical involved is directly affected by the absorption in the visible range. In addition, UV-Vis spectroscopy is very important for the quantitative measurements despite its limitations for sample identification. Furthermore, the absorbance measurements allow determining the analyte concentration. The characterization of the optical and/or the electronic properties of materials is usually based on their UV-Vis spectra [31-33].

The aim of this study is to find the E_g value in one step. As the transmittance curves in the materials yield a lot of information, the analytical model proposed here is based on the transmittance curve to easily calculate the E_g value. In addition, we carefully checked the values obtained with other results.

The novelty of this work is the development of an analytical model providing a new unified formula of E_g . This new formula will enable liable reading of the E_g for several samples. For this reason, test examples were considered which were based on the deposition and characterization of thin layers.

EXPERIMENTAL

Preparation of thin film samples

Before starting the development of the energy gap formula; we shall briefly present the experimental preparation of thin conductive and transparent layers of ZnO. Different solution concentrations were prepared by spray pyrolysis processing of glass substrates with fluorine-doped tin oxide (FTO). These films were obtained from a solution of zinc acetate dissolved in methanol at a fixed temperature ($T=350^\circ\text{C}$) and with different concentrations of the solution in the range from 0.1 M to 0.5 M.

The different solution concentrations led to the variation of the structural and optical properties of these films.

The UV-Vis spectrophotometric measurements confirmed that good transparencies with a transmission of 70 - 85% in the visible range can be obtained. The values of the optical band gaps E_g deduced from the transmission UV-Vis spectra varied between 3.24eV and 3.43eV [34-36].

For this reason, our work focused on the calculation of the E_g value. Figure 1 shows the

transmission UV-Vis spectra of ZnO/FTO layers at different concentrations. It is clear that the energy gap will be different from one layer to another.

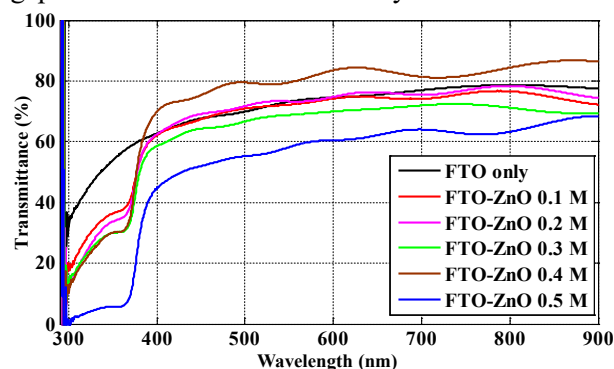


Fig. 1. Transmission spectra of ZnO/FTO samples for different molar concentrations.

Measurements

The fields of spectroscopy are generally distinguished according to the wavelength interval in which the measurements are made. The following characterization domains can be distinguished: ultraviolet-visible, infrared, microwave, etc.

In this case, we used a UV-Vis spectrophotometer, whereby we were able to plot curves representing the variation in the transmittance depending on the wavelength in the UV-Vis range of 300-900 nm (see Fig. 1). By exploiting these curves it is possible to estimate several quantities of the film such as thickness, optical characteristics, optical absorption threshold, absorption coefficient, width of the forbidden band and refractive index.

Our proposed approach here is to determine the energy gap value using the transmittance spectra. The next section will try to present the calculation in detail.

Analytical model of energy gap calculation

Everything in nature is subject to the laws that govern it. We therefore thought of a law to determine the energy gap (E_g) value based on the transmittance curves. There are some almost aligned points in the UV-Vis field that would build a straight line. The intersection between the line and the curve above is denoted as point B, and below is point A.

Theoretically, the line formed is parallel to the transmittance axis and perpendicular to the wavelength axis. But in reality the straight line is inclined, that is to say, $\lambda_B \neq \lambda_A$.

Point B is projected on the horizontal line which passes through point A; we denote this new point by C. Points B and C have the same wavelength λ_B

(see Fig. 2).

Some researchers in this field take the E_g in point B; but other researchers take it in point A [37-41]. This led us to develop a realistic formula for defining E_g and comparing the results obtained between the practical and the theoretical values.

The triangle ACB is right angled at C; we determined the center of gravity G of the triangle (see Fig. 2).

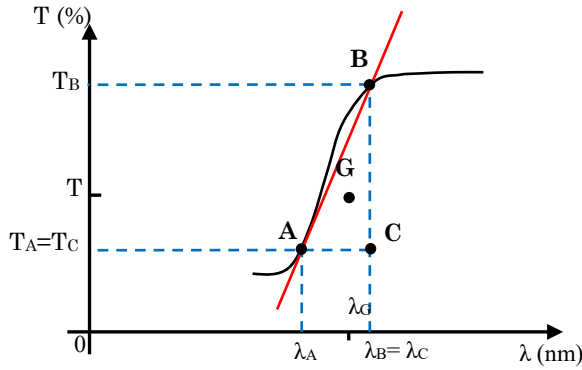


Fig. 2. Illustrative scheme of the transmission spectra.

According to Fig. 2, we assume that the points A, B, C of the triangle have equal masses m . By applying the law of the gravity center which is given by:

$$\overline{OG} = \frac{m\overline{OA} + m\overline{OB} + m\overline{OC}}{m + m + m} \quad (1)$$

or,

$$\overline{OG} = \frac{\overline{OA} + \overline{OB} + \overline{OC}}{3} \quad (2)$$

we can also write,

$$\overline{OA} = \lambda_A \times \vec{i} + T_A \times \vec{j} \quad (3)$$

$$\overline{OB} = \lambda_B \times \vec{i} + T_B \times \vec{j} \quad (4)$$

$$\overline{OC} = \lambda_B \times \vec{i} + T_A \times \vec{j} \quad (5)$$

so,

$$\overline{OG} = \frac{(\lambda_A + 2\lambda_B)}{3} \times \vec{i} + \frac{(2T_A + T_B)}{3} \times \vec{j} \quad (6)$$

We are interested in the part of the wave axis. The wavelength λ_G of the gravity center is written in this case as follows:

$$\lambda_G = \frac{(\lambda_A + 2\lambda_B)}{3} \quad (7)$$

It is known that:

$$E_g = \frac{1240}{\lambda} \quad (8)$$

According to equation (7) which defines the wavelength λ_G , we can extract the wavelength λ which is introduces in the calculation of E_g value

by:

$$\lambda = \lambda_G = \frac{(\lambda_A + 2\lambda_B)}{3} \quad (9)$$

so,

$$E_g = \frac{1240}{\lambda} = \frac{1240}{\frac{(\lambda_A + 2\lambda_B)}{3}} = \frac{3720}{(\lambda_A + 2\lambda_B)} \quad (10)$$

The final formula for determining the E_g value is:

$$E_g = \frac{3720}{(\lambda_A + 2\lambda_B)} \quad (11)$$

This method allows us to determine the energy gap (E_g) value based on the transmittance curve simply, efficiently and closer to the previous results.

We have demonstrated by mechanical laws at the beginning that we consider the selected points as mass centers and we have determined the center of mass of the proposed system in order to have a unified formula of the E_g .

It is important to facilitate the calculation of the E_g value in the subjects that use the transmittance curves in materials intended for photovoltaic systems or other uses.

The proposed analytical model based on the transmittance curve permits easy calculation of the E_g value. In addition, we have carefully checked the values obtained with other results. Equation (11) gives a new formula which was found according to well-defined steps.

Applying the new formula on a real example (ZnO/FTO)

In Fig. 3 we present the transmittance spectra of the ZnO/FTO films at a concentration of 0.4 M.

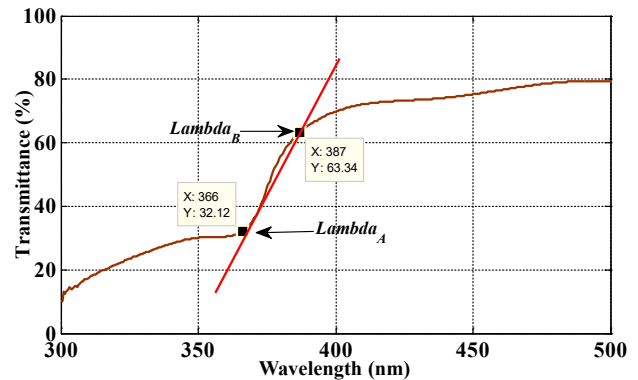


Fig. 3. Transmission shape of ZnO/FTO for 0.4 M concentration.

The band gap or energy gap (E_g) values of our ZnO/FTO layers are between 3.24 and 3.43 eV. According to Fig. 1, we can see a variation of the E_g value with the concentration of the solution. For the concentration of 0.4 M presented in Fig. 3;

the E_g value agrees with the literature value [34-36].

$$E_g = \frac{3720}{(366 + 2 \times (387))} = \frac{3720}{1140}$$

so,

$$E_g = 3.263 \text{ eV}.$$

Note: In this occasion, we can define another formula that is based on the calculation of the average value of each E_g value, as follows:

$$E_{gA} = \frac{1240}{\lambda_A} \quad (12)$$

and,

$$E_{gB} = \frac{1240}{\lambda_B} \quad (13)$$

$$E_{g-Mean} = E_g = \frac{E_{gA} + E_{gB}}{2} \quad (14)$$

or,

$$E_{g-Mean} = E_g = 620 \times \frac{(\lambda_A + \lambda_B)}{(\lambda_A \times \lambda_B)} \quad (15)$$

In this case, we can find the E_g value as follows:

$$E_{g-Mean} = E_g = 620 \times \frac{(366 + 387)}{(366 \times 387)}$$

so,

$$E_{g-Mean} = E_g = 3.269 \text{ eV}$$

It is clear that the two values are not equal (3.263 eV vs. 3.269 eV). For this reason, our analytical model shows a very good approximation when comparing with literature values[42-44].

Applying the new formula on a real example (NiO /FTO)

Before starting to calculate the energy gap based on the previous formula., we shall firstly indicate the experimental preparation of thin conductive and transparent layers of NiO. Different solution concentrations were prepared by spray pyrolysis processing on glass substrates with fluorine-doped tin oxide (FTO). These films were obtained from a solution of nickel nitrate in methanol at a fixed temperature ($T = 480^\circ\text{C}$) and with different concentrations (from 0.1 M to 0.5 M).

Fig. 4 shows the UV-Vis transmittance spectra of NiO/FTO layers at different concentrations. It is clear that the energy gap will be different from one layer to another. The band gap or energy gap (E_g) values of our NiO/FTO layers are between 3.38 eV and 3.74 eV. According to Fig. 4, there is a variation of the E_g value with the concentration of the solution.

For a concentration of 0.2 M presented in Fig. 4 (to the left); the $E_g = 3.68 \text{ eV}$ value agrees with the

literature value [45-47].

$$E_g = \frac{3720}{(319.3 + 2 \times (345.4))} = \frac{3720}{1010.1}$$

so,

$$E_g = 3.68 \text{ eV}$$

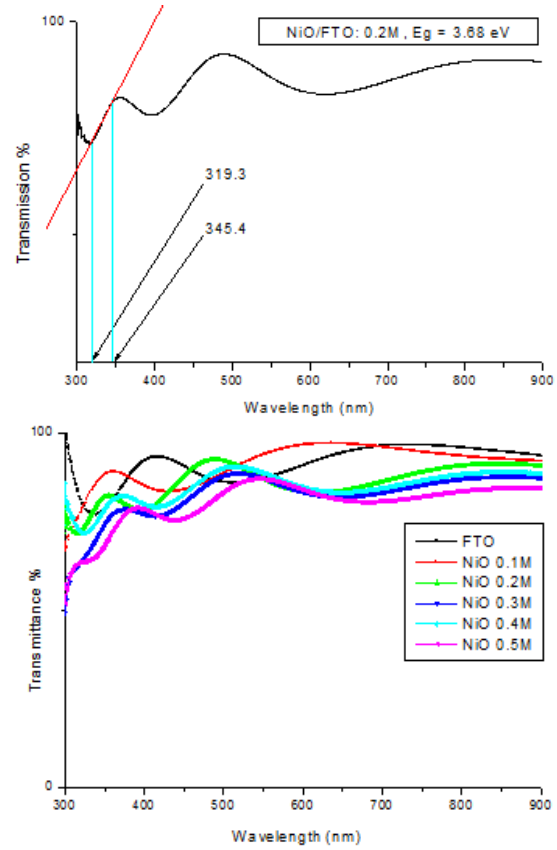


Fig. 4. Transmittance spectra of FTO only and of NiO thin films grown on FTO substrates at various solution concentrations.

Based on the calculation of the average value of each energy gap value, we can find the results as follows:

$$E_{gA} = \frac{1240}{\lambda_A} = 3.59 \text{ eV}$$

and,

$$E_{gB} = \frac{1240}{\lambda_B} = 3.8835 \text{ eV}$$

$$E_{g-Mean} = E_g = \frac{E_{gA} + E_{gB}}{2}$$

or,

$$E_{g-Mean} = E_g = 620 \times \frac{(\lambda_A + \lambda_B)}{(\lambda_A \times \lambda_B)}$$

In this case, we can find the E_g value as follows:

$$E_{g-Mean} = E_g = 620 \times \frac{(319.3 + 345.4)}{(319.3 \times 345.4)}$$

so,

$$E_{g-Mean} = E_g = 3.736 \text{ eV}$$

Table 1. Energy gap values at different NiO concentrations

NiO Concentration	0.1M	0.2M	0.3M	0.4M	0.5M	FTO
E_g for Classical Method (eV)	3.93	3.92	3.86	3.79	3.75	3.67
E_g for New Method (eV)	3.74	3.68	3.57	3.52	3.38	3.62
Error = $(E_{g\text{Measured}} - E_{g\text{Classical}}) / E_{g\text{Classical}}$	0.04	0.06	0.07	0.07	0.09	0.01

The comparison of the energy gap values for solution concentrations between 0.1 and 0.5M based on the classical method and on the new formula is shown in Table 1. It is seen that the results obtained are in good agreement with the results of the conventional calculation method. We can mention the difference of 5% between the estimated value and the conventional value for pure FTO. This difference varies in the range from 0.19eV to 0.37eV depending on the NiO concentration from 0.1M to 0.5M. This small variation can be justified by the position of the tangent line which is seen as a challenge to improve this analytical model. Generally, the results clearly show the ease of calculating the E_g value based on a single formula.

It is also important to note that the verification was made for other materials such as ITO, CuO, etc. and confirmed the accuracy of the proposed model.

DISCUSSION

Pankove [49] proposed a technique based on traced optical absorbance data to determine the energy gap. The work of Tauc *et al.*[48] was applied to the study of the optical and electronic properties of amorphous germanium. The Tauc diagram is a graph commonly used to determine the optical band gap of a material, usually a semiconductor. The optical band gap can be determined using the Tauc's relation [48, 49] which is given by:

$$(\alpha h\nu)^p = A(h\nu - E_g) \quad (16)$$

where, α is the absorption coefficient, h is the Planck's constant, A is a constant, ν is the transition frequency, E_g is the band gap corresponding to a particular transition occurring in the film and p can take values according to:

- Direct allowed transitions: $p=2$,
- Direct forbidden transitions: $p=2/3$,
- Indirect allowed transitions: $p=1/2$,
- Indirect forbidden transitions: $p=1/3$.

Generally, the allowed transitions dominate based on the absorption processes, so, $p=2$ or $p=1/2$, in case when the transitions are direct or indirect, respectively.

This new approach has led us to find a well-defined formula of the E_g value. The logical steps during the demonstration confirm the accuracy of the results. In addition, the examples proposed in this study illustrate the effectiveness of this formula when we compare it with other works [40, 41, 50, 51].

In this paper, we have tried to put forward a new approach that helps to avoid the overlap in the E_g calculation.

CONCLUSIONS

In conclusion, we proposed a new analytical model based on the transmittance curve in order to calculate the E_g value. This study was based on real examples to calculate the E_g value. Examples were composed of thin film samples which contained ZnO/FTO or NiO/FTO. In addition, we carefully checked the values obtained with other results. We found the value of $E_g = 3.263$ eV in the ZnO/FTO example; this value is in correspondence with the literature. So, equation (11) gives a new formula developed according to well-defined steps.

Finally, it may be important to facilitate the calculation of the E_g value in subjects that use the transmittance curves.

Acknowledgements: This paper was partially supported by VTRS laboratory at the University of El-Oued, Algeria. We thank all colleagues in the VTRS laboratory for any help to us.

REFERENCES

1. P. Mishra, R. S. Yadav, A. C. Pandey, *Bulg. Chem. Commun.*, **42**, 560 (2010).
2. S. I. Gudkov, K. D. Baklanova, M. V. Kamenshchikov, A. V. Solnyshkin, A. N. Belov, *Phys. Solid. State*, **60**, 4 (2018).
3. Y. Takeshi, J. Kaji, K. Koda, K. Takashima, M. Nakano, H. Fukunaga, *IEEE Trans. Mag.*, **54**, 11 (2018).
4. N. G. Kostova, M. Fabian, E. Dutkova, *Bulg. Chem. Commun.*, **51**, 433 (2019).
5. B. Swati, N. Lohia, D. Rehani, S. Mehra, R. Datt, G. Gupta, D. Haranath, S. Sharma, *Opt.*, 164015 (2019).
6. M. Cheng, Z. B. Chen, J. W. Xing, *IEEE Trans. Mag.*, **54**, 5 (2018).

7. D. Selloum, A. Henni, A. Karar, A. Tabchouchea, N. Harfoucheb, O. Bachaa, S. Tingryc, F. Roseid, *Solid State Sciences*, **92**, 76 (2019).
8. N. Kaneva, A. Bojinova, K. Papazova, D. Dimitrov, *Bulg. Chem. Commun.*, **51**, 406 (2019).
9. I. A. Tambasov, M. N. Volochaev, A. S. Voronin, N. P. Evsevskaia, A. N. Masyugin, A. S. Aleksandrovskii, T. E. Smolyarova, *Phys. Solid. State*, **61**, 10 (2019).
10. M. Sadullah, J. Kaur, R. Basu, A. K. Sharma, *Opt.* 163715 (2019).
11. A. Shokri, K. Mahanpoor, *Bulg. Chem. Commun.*, **50**, 27 (2018).
12. C. Sungju, J. Y. Kim, J. Rhee, H. Kang, S. Park, D. M. Kim, S. J. Choi, D. H. Kim, *IEEE Elect. Dev. Lett.*, **40**, 4 (2019).
13. A. Henni, N. Harfouche, A. Karar, D. Zerrouki, F. X. Perrin, F. Rosei, *Solid State Sciences*, **98**, 106039 (2019).
14. W. Rakhrou, D. Selloum, A. Henni, N. Cherrad, I. Chikouche, M. Benalia, S. Mouffok, M. Djedid, N. Bouzar, S. Tingry, *J. Inorg. Organomet. Polym. and Mat.*, **31**, 62 (2021).
15. B. A. Belyaev, N. A. Drokin, V. A. Poluboyarov, *Phys. Solid. State*, **60**, 2 (2018).
16. A. L. Diaz, M. R. Cabello, J. Alvarez, A. R. Bretones, S. G. Garcia, *IEEE Trans. Mic. Theor. Tech.*, **66**, 2 (2018).
17. S. Zhang, H. D. Hadi, Y. Wang, B. Liang, V. T. Tiong, F. Ali, Y. Zhang, T. Tesfamichael, L. H. Wong, H. Wang, *IEEE Jour. Photov.*, 3 (2018).
18. M. E. Kompan, Y. P. Stepanov, *Phys. Solid. State*, **56**, 6 (2014).
19. H. Y. Liu, C. C. Hung, W. C. Hsu, *IEEE Elect. Dev. Letters*, **39**, 10 (2018).
20. F. Lisco, P. M. Kaminski, A. Abbas, K. Bass, J. W. Bowers, G. Claudio, M. Losurdo, J. M. Walls, *Thin Solid Films*, **582**, (2015).
21. Y. M. Kim, H. B. Kang, G. H. Kim, C. S. Hwang, S.-M. Yoon, *IEEE Elect. Device Letters*, **38**, 10 (2017).
22. M. Etminan, N. S. Hosseini, N. Ajamgard, A. Koohian, M. Ranjbar, *Optik*, **199**, 163517 (2019).
23. M. A. Chergui, D. Djouadi, B. Benhaoua, A. Chelouche, M. Boudissa, *Optik*, **180**, (2019).
24. M. J. Park, J. Y. Jung, S. M. Shin, J. W. Song, Y. H. Nam, D. H. Kim, J. H. Lee, *Thin Solid Films*, **599**, (2016).
25. P. R. Dilber, L. B. Chandrasekar, N. M. S. S. Bathusha, R. Chandramohan, M. Karunakaran, S. R. Srikumar, *Phys. Solid State*, **60**, 5 (2018).
26. Y.J. Jia, W.X. Su, Y.B. Hu, H.N. Chen, *Bulg. Chem. Commun.*, **49**, 190 (2017).
27. S. Krishnaswamy, V. Ragupathi, S. Raman, P. Panigrahi, G. S. Nagarajan, *Optik*, **194**, (2019).
28. S. T. Zhang, G. Vitrant, E. Pernot, C. Jiménez, D. M. Rojas, D. Bellet, *Nanomaterials*, **8**, 6 (2018).
29. M. A. Sulimov, M. V. Yakushev, I. Forbes, J. M. Prieto, A. V. Mudryi, J. Krustok, P. R. Edwards, R. W. Martin, *Phys. Solid State*, **61**, 5 (2019).
30. M. Tani, Y. Kawamura, M. Horita, Y. Ishikawa, Y. Uraoka, IEEE, Osaka, 2011, p. 84.
31. A. Zaiour, A. Benhaya, T. Bentrchia, *Optik*, **186**, (2019).
32. R. Sharma, S. L. Patel, S. Chander, M. D. Kannan, M. S. Dhaka, *Phys. Letters*, **384**(24), 126557 (2020).
33. S. Tomita, S. Hayashi, Y. Tsukuda, M. Fujii, *Phys. Solid State*, **44**, 3 (2002).
34. H. Slimani, N. Bessous, S. Dagher, A. Hilal-Alnaqbi, M. El Gamal, B. Akhozheya, M. Mohammed, *Materials Research Express*, **2**, 025026 (2020).
35. N. Kamarulzaman, M. F. Kasim, R. Rusdi, *Nano Research Letters*, **10**, 1 (2015).
36. V. Srikant, D. R. Clarke, *J. Appl. Physics*, **83**, 5447 (1998).
37. A. Sáenz-Trevizo, P. Amézaga-Madrid, P. Pizá-Ruiz, P. Pizá-Ruiza, W. Antúnez-Flores, M. Miki-Yoshida, *Materials Research*, **19**, 33 (2016).
38. Z. Jalil, M. I. Bukhari, *Journal of Physics: Conference Series. IOP Publishing*, 032020 (2018).
39. A. Arif, O. Belahssen, S. Gareh, S. Benramache, *Journal of Semiconductors*, **36**, 013001 (2015).
40. F. K. Shan, Y. S. Yu, *J. Europ. Ceramic Society*, **24**, 1869 (2004).
41. N. Guermat, W. Daranféd, K. Mirouh, *Ann. Chimie Sci. Materiaux*, **44**, 347 (2020).
42. S. Marouf, A. Beniaiche, H. Guessas, A. Azizi, *Materials Research*, **20**, 88 (2016).
43. N. Hacini, M. Ghamnia, M. A. Dahamni, A. Boukhachem, J. Pireaux, L. Houssiau, *Coatings*, **11**, 202 (2021).
44. N. Shakti, P. S. Gupta, *Appl. Physics Research*, **2**, 19 (2010).
45. K. O. Ukoba, A. C. Eloka-Eboka, F. L. Inambao, *Renewable and Sustainable Energy Reviews*, **82**, 2900 (2018).
46. F. Hajakbari, M. T. Afzali, A. Hojabri, *Acta Phys.*, **131**, 417 (2017).
47. A. Echresh, M. A. Abbasi, M. Z. Shoushtari et al. *Semicond. Science and Tech.*, **29**, 115009 (2014).
48. J. Tauc, R. Grigorovici, A. Vancu, *Phys. Status Solidi*, **15**, (1966).
49. J. I. Pankove, *Optical Processes in Semiconductors*, Dover Publications, Inc., New York, 1971.
50. B. D. Viezbicke, S. Patel, B. E. Davis, D. P. Birnie, *Phys. Status Solidi*, **252**(8), 1700 (2015).